



# An enhanced poly(vinylidene fluoride) matrix separator with TEOS for good performance lithium-ion batteries

Jiuqing Liu<sup>1</sup> · Cheng Wang<sup>1</sup> · Xiufeng Wu<sup>1</sup> · Fangfang Zhu<sup>1</sup> · Meng Liu<sup>1</sup> · Yang Xi<sup>1</sup>

Received: 12 June 2018 / Revised: 26 September 2018 / Accepted: 12 October 2018 / Published online: 25 October 2018  
© The Author(s) 2018

## Abstract

The low crystallinity poly(vinylidene fluoride)/tetraethyl orthosilicate silane (PVDF/TEOS) composite separator with a finger-like pore structure for lithium-ion battery has been successfully prepared by non-solvent-induced phase separation (NIPS) technique. The PVDF/TEOS composite separator shows the excellent wettability and electrolyte retention properties compared with Celgard 2320 separator. AC impedance spectroscopy results indicate that the novel PVDF/TEOS composite separator has ion conductivity of  $1.22 \text{ mS cm}^{-1}$  at  $25 \text{ }^\circ\text{C}$ , higher than that of Celgard 2320 separator ( $0.88 \text{ mS cm}^{-1}$ ). The lithium-ion transference number of PVDF composite separator added 0.7% TEOS was 0.481, better than that of Celgard 2400 (0.332). What is more, the lithium-ion batteries assembled with PVDF/TEOS composite separator show good cycling performance and rate capability.

**Keywords** Separator · Phase inversion · PVDF/TEOS · Lithium-ion battery

## Introduction

Scientists and engineers have long believed in the promise of batteries to change the world. The ubiquitous battery has already come a long way, especially lithium-ion batteries. Owing to their high energy density and outstanding cycle life, lithium-ion batteries are now widely employed in commercial electronics, and also furthered into surging markets such as electrical vehicles [1]. Separator, which is sandwiched between the cathode and the anode to prevent the physical contact of the electrodes while enabling free ionic transport and electronic flow, directly affects the interface structure [2], the internal resistance [3–5], the battery capacity [2, 3, 6–11], cycle characteristics [12], and safety performance. Essentially, a separator should be chemically and electrochemically stable toward the electrolyte and electrode materials and must be mechanically strong enough to withstand handling during battery assembly; moreover, it should have sufficient porosity to absorb liquid electrolyte for high ionic conductivity. The most common separator materials used in

lithium-ion batteries are polyethylene (PE) and polypropylene (PP). They have good mechanical stress property and polypropylene (PP) separator has good thermodynamic stability. In addition, the  $\text{SiO}_2/\text{PVDF}$  composite separator combined with the good mechanical strength of PP nonwoven has been prepared and applied to lithium-ion batteries [13]. The addition of nanocrystalline cellulose (NCC) has improved the electrolyte retention and storage modulus of PVDF-HFP composite separator [14]. What's more, the single ion polymer electrolyte which is comprised of polymeric lithium tartaric acid borate salt (PLTB) and PVDF-HFP has been used to improve cellulose composite separator. The enhanced composite separator shows higher ionic conductivity, good flame retardancy, and superior thermal resistance compared to the commercial polypropylene (PP) separator [15]. However, the polyethylene (PE) and polypropylene (PP) separators have low porosity, poor wettability with polar liquid electrolyte, and large thermal shrinkage at high temperatures. These drawbacks affect cell resistance, energy density, rate capability, and safety of lithium-ion batteries [12, 16–18].

A promising way to overcome these problems is using room temperature ionic liquids (RTILs), which has several attractive features, such as chemical and thermal stability, non-volatility, and intrinsic high ionic conductivity at room temperature which results in the improved safety in case of overcharging. Recently, gel polymer-based electrolytes

✉ Jiuqing Liu  
jiuqing\_liu@163.com

<sup>1</sup> School of Metallurgy and Environment, Central South University, Changsha 410083, Hunan, China

(GPE), including polyethylene oxide (PEO) [10], cellulose [11], polyacrylonitrile (PAN) [12], poly(vinylidene fluoride-co-hexafluoropropylene) (PVDF-HFP) [16], and poly(vinylidene fluoride) (PVDF) [17], have been widely investigated, because of their high ionic conductivity, electrochemical stability, and electrolyte wettability.

But the poor strength of GPE hindered the application in batteries [18]. Due to the strong electron-withdrawing functionality in C–F in the molecular structure, PVDF becomes one of the typical polymers which are used as the gel polymer separator [19]. The connectivity of pore and crystallinity of PVDF separators contribute to the lithium-ion conductivity, because the well-interconnected pore can reduce the distance of ion migration and the lower crystallinity can improve the area of amorphous domain [20]. However, the mechanical stress and ion conductivity could not afford the requirements of power batteries.

Composite separators combine the advantages of GPE and polyolefin separators. They have good mechanical stress property, wettability, and electrolyte retention properties. Researchers work on the preparation of composite separator and investigate the properties of different composite separators, but the structure of composite layers has not been investigated. In this paper, PVDF/Celgard 2320 composite separator with a novel finger-like pore structure has been prepared by non-solvent-induced phase separation (NIPS) method. In addition, PVDF composite layer with low crystallinity is obtained by adding tetraethyl orthosilicate silane (TEOS).

## Experimental

### Preparation of PVDF/TEOS composite separator

Twelve grams pristine PVDF (PVDF, HSV900, Arkema Inc.  $M_w = 1000,000 \text{ g mol}^{-1}$ ) and 1 g polyvinyl pyrrolidone (PVP, K30, Damao Chemical Reagent Co., Ltd., Tianjin, China) were mixed in 86.8 g N,N-Dimethylacetamide (DMAc, Sinopharm Chemical Reagent Co., Ltd., Ningbo, China) in a

conical flask with continuously stirring. Then, 0.2 g TEOS (Sinopharm Chemical Reagent Co., Ltd., Ningbo, China) was added into the conical flask. The mixture was continuously stirred at 70 °C for 12 h to obtain the homogeneous casting solution. Then the conical flask containing the homogeneous casting solution was stoppered and placed in a vacuum oven at 70 °C overnight to eliminate the air bubbles. Composite separator was prepared by coating process; thereafter, the casting solution was cast on Celgard 2320 by a home-made casting knife. The thickness of PVDF layer was about 10  $\mu\text{m}$ . The wet composite separator was left in air for 10 s at 25 °C and was then immersed into the mixing coagulation bath ( $W_t \text{ deionized water} : W_t \text{ DMAc} = 8:2$ ) for 12 h. The resulting separator was immersed into deionized water for 3 days to remove the residue solvent. Finally, the composite separator was dried in vacuum oven at 50 °C for 12 h to remove the residue water.

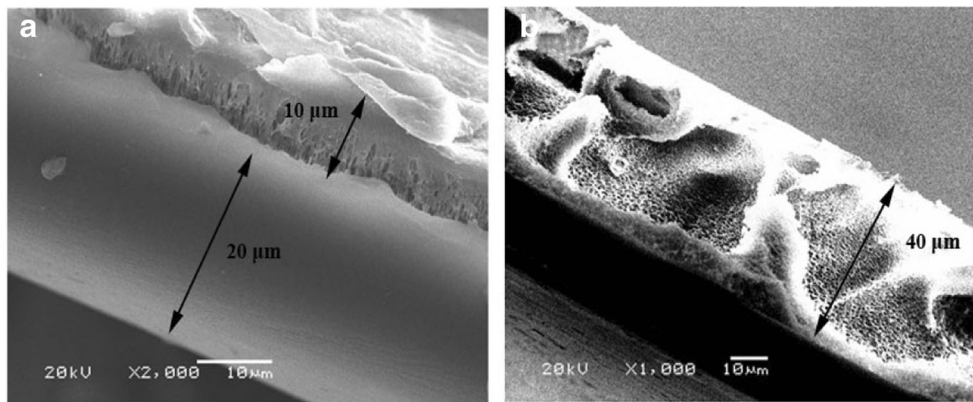
### Electrode preparation and cell assembly

A cathode slurry comprising 80% LiCoO<sub>2</sub> (Hunan Shanshan Battery Materials Co. Ltd., China), 10% PVDF (Aladdin,  $M_w = 150,000 \text{ g mol}^{-1}$ ), 10 wt% carbon black (Super P, Timcal), and N-methyl-1-pyrrolidone (NMP, Aldrich) were casted on aluminum foil by using a doctor blade and dried at 60 °C for 12 h. A lithium metal was used as counter electrode in this study. Half cells (CR2025-type coin cell) were assembled by sandwiching the prepared membranes between a LiCoO<sub>2</sub> cathode and a lithium metal within an argon-filled glove box (Universal 2440/750) with a low moisture level (< 1 mg L<sup>-1</sup>). The liquid electrolyte was 1.0 M LiPF<sub>6</sub>-ethylene carbonate (EC)/dimethyl carbonate (DMC)/ethyl methyl carbonate (EMC) (1:1:1, v/v/v) (Duoduo Reagent Co. Ltd., China).

### Material characterization

The ionic conductivity ( $\delta$ , mS cm<sup>-1</sup>) was evaluated by AC impedance spectroscopy in a frequency range from 10<sup>-2</sup> to 10<sup>-6</sup> Hz with 5 mV of AC amplitude at 25 °C. The separators

**Fig. 1** Cross section of pristine PVDF/PP composite separators with different composite layer thicknesses (the composite layer thickness in **a** is 10  $\mu\text{m}$  and the composite layer thickness in **b** is 40  $\mu\text{m}$ )



(electrolyte soaked) were sandwiched between two stainless steels (SS, diameter = 16.2 mm) which were assembled in CR2025-type coin cells. The cell assembly was also done in the glove box with argon gas of low water content. The ionic conductivity was calculated as Eq. (1):

$$\delta = \frac{l}{R_b \times A} \tag{1}$$

where  $R_b$  is the bulk resistance of the electrolyte and the intercept of the  $Z'$ -axis of the straight line, and  $l$  and  $A$  are the thickness and area of the separator disk, respectively.

The electrolyte uptake was measured by immersing the separator in the liquid electrolyte at 25 °C for 30 min. Then the liquid electrolyte-soaked separator was taken out and weighed quickly on a microbalance after removing the excess

surface solution with wipes. Liquid electrolyte uptake was calculated as Eq. (2):

$$Eu(\%) = \frac{W_1 - W_0}{W_0} \times 100\% \tag{2}$$

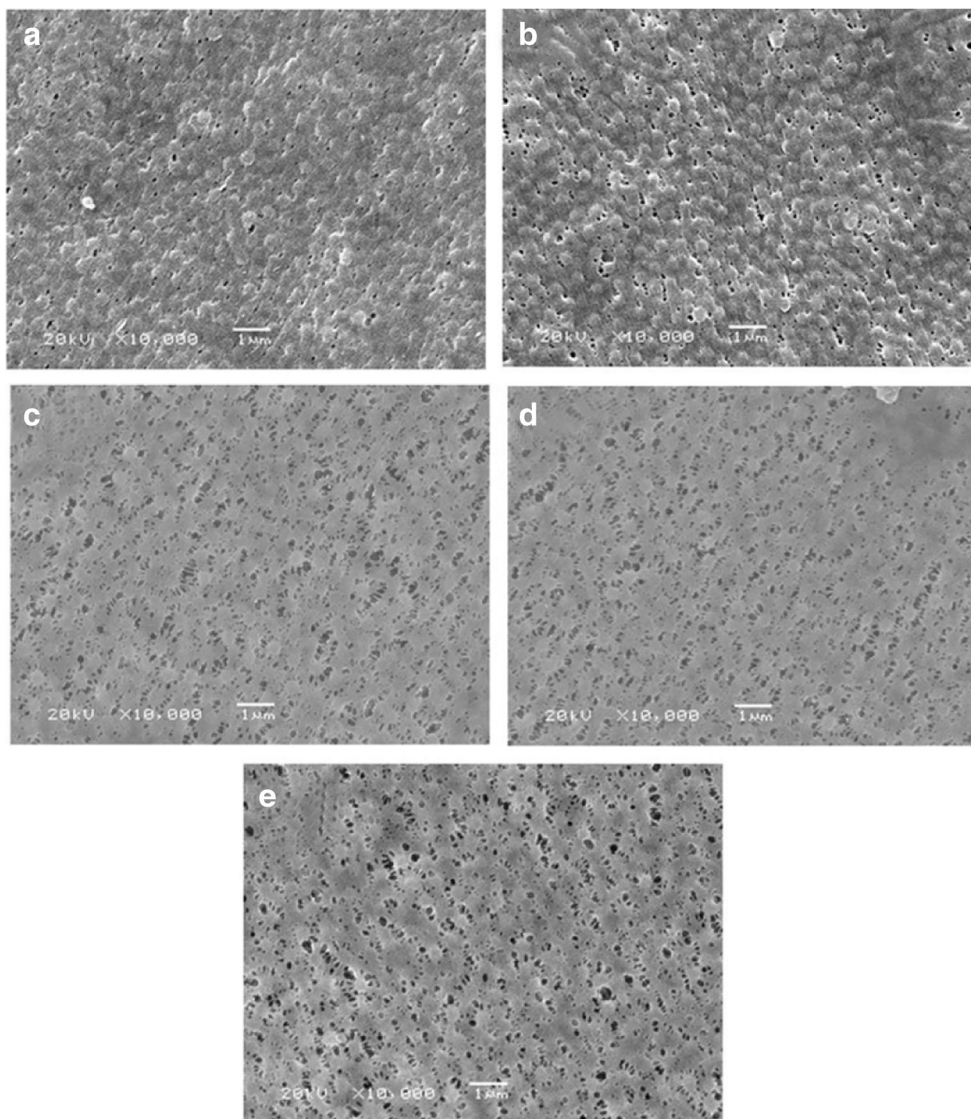
where  $Eu$  is the PVDF liquid electrolyte uptake, and  $W_0$  and  $W_1$  are the weight of separators before and after soaked in liquid electrolyte, respectively.

The porosity of a separator has a large influence on the electrolyte uptake and wettability of the separator. The porosity of separator was calculated as Eq. (3):

$$Porosity(\xi) = 1 - \frac{m}{\rho v} \tag{3}$$

where  $m$  is the weight of PVDF, while  $\rho$  and  $v$  represent the density of PVDF and the volume of the separator, respectively.

**Fig. 2** SEM images of the top surface of the PVDF/TEOS composite separator (a, b, c, d, and e represent PVDF/TEOS composite separator with 0.1%, 0.3%, 0.5%, 0.7%, and 1.0% TEOS additions, respectively)



Lithium-ion transference number is one of the important indicators for evaluating battery performance. The lithium-ion transference number was calculated as Eq. (4):

$$T_+ = \frac{I^{ss}}{I^0} \quad (4)$$

where  $T_+$  is the lithium-ion transference number, while  $I^0$  represents the polarization start current and  $I^{ss}$  represents the polarization steady-state current, respectively. By assembling a symmetrical analog battery which has a structure of lithium sheet/polymer electrolyte separator/lithium sheet,  $I^0$  and  $I^{ss}$  of the analog battery can be measured by a frequency response analyzer (FRA, CHI660D, Shanghai).

Morphology of composite separators after cycled at 1 C rate for 300 cycles was studied by scanning electron microscope (SEM, JSM5600L, Japan). Crystallinity of composite separators was investigated by X-ray diffraction (XRD, Rint2000, Japan).

Thermogravimetric analysis (TGA) of the separators was carried out by 704 F1 Phoenix. The samples were tested in an argon atmosphere at a heating rate of  $5\text{ }^\circ\text{C min}^{-1}$ .

The diffuse reflectance infrared spectrometry (DRIFT) was employed to measure the infrared spectra (IR) of the samples in the range of  $400\text{--}4000\text{ cm}^{-1}$  with the resolution  $2\text{ cm}^{-1}$  on a BRUKER VECTOR-22 spectrometer.

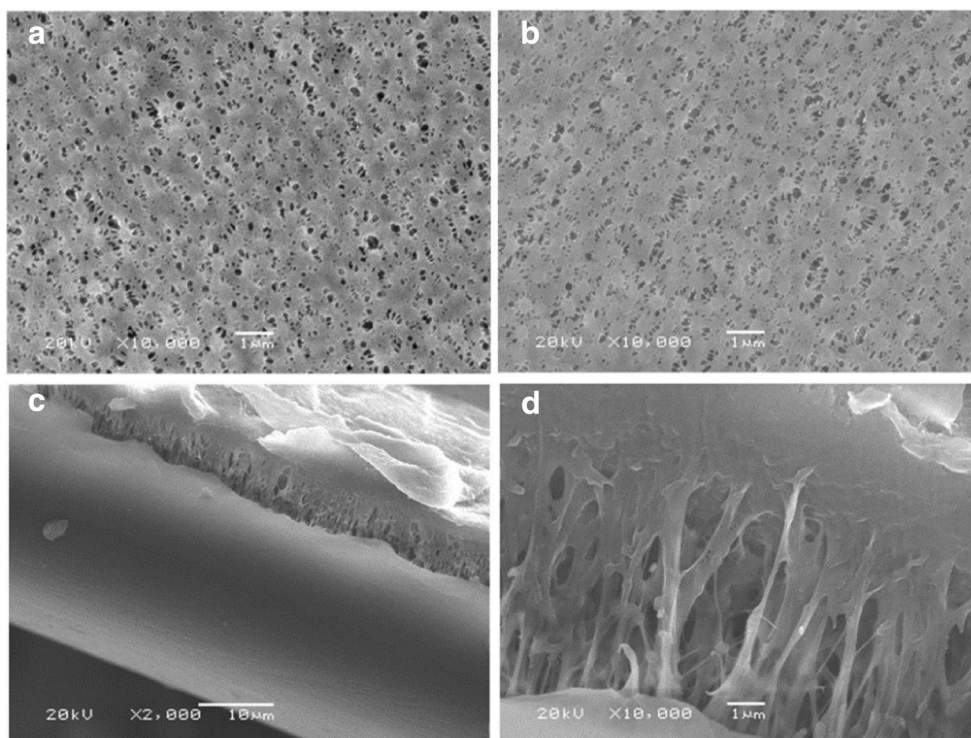
The half cells were assembled in an argon-filled glove box and sealed in 2025-type coin cells. Galvanostatic charge/discharge cycling was performed at voltage range of 3.0–

4.3 V in a Neware Battery Test System (Shenzhen Neware New Energy Tech. Co. Ltd).

## Results and discussion

The morphology of porous PVDF separator prepared by non-solvent-induced phase separation technique has a different pore structure with different thickness. Figure 1 shows SEM images of the cross section of PVDF composite separators with different composite layer thickness, from which it can be seen that the morphology of PVDF composite layer is close to that of the pristine PVDF. According to Fig. 1a, the thickness of the PVDF composite layer is about  $10\text{ }\mu\text{m}$ , and the pore structure is narrow and long. With the thickness of composite layer increasing to  $40\text{ }\mu\text{m}$  as shown in Fig. 1b, the macrovoids combined with the typical finger-like structure was obtained. From the SEM micrographs of cross section of these separators, it is found that the thinner composite layer tends to precipitate in the finer and narrow structure, while the thicker composite layer leads to form the finger-like structure. This may be related with the solvent in casting solution exchanged with the non-solvent in coagulation bath due to diffusion, which results in the liquid-liquid phase separation into a polymer-rich phase and a polymer-poor phase. The liquid-liquid phase separation continues to form the porous structure until the polymer-rich phase is solidified by gelation [18]. Consequently, it can be concluded that the effect of the

**Fig. 3** SEM images. **a** The top surface of the pristine PVDF composite separator. **b** The top surface of the PVDF/TEOS composite separator. **c** The cross section of PVDF/TEOS composite separator. **d** The finger-like pore structure of PVDF/TEOS composite separator



composite layer with different thickness on the pore structure is due to the penetration of the solution through the bottom of PP pores and the occurrence of phase separation process when the PP separator coated with the PVDF casting solution is immersed into the mixing coagulation bath. The phase separation process is dominated by the mixing coagulation bath that permeates from the bottom of PP pores when the PVDF composite layer is thinner. The coagulation bath solution mainly enters the PVDF layer from the upper surface of the separator for exchange which is similar to the phase exchange process of a single-layer PVDF separator when the PVDF composite layer is thicker, at the same time, the coagulation bath solution also seeps into the PVDF composite layer from PP separator; thus, the finger-like pores in the PVDF composite layer are very large. Excessive composite separator thickness increases the separator resistance; therefore, the thickness of PVDF composite layer of the composite separator prepared in this paper is controlled at about 10  $\mu\text{m}$ .

In order to investigate the morphology of the composite separators, a series of PVDF/TEOS composite separator were prepared with TEOS content varying from 0.1 to 1.0 wt%. Figure 2 shows the SEM micrographs of the modified separator surface, and it is found that the pore size of PVDF composite layer increases slightly with TEOS content increasing. Moreover, as is shown in Fig. 2, the composite separator has a more uniform surface pore structure than pristine PVDF. The uniform distribution of pore contributes to the battery performance because the non-uniform distribution of pore leads to the non-uniform current density and the active materials which come in contact with the high-porosity regions would have to work harder and invalid [21].

As shown in Fig. 3a, b, the PVDF composite separator has a very smooth surface with the uniform micro-pore structure and the pore size is about 0.2  $\mu\text{m}$ . In the presence of TEOS, the pore size of composite separator becomes smaller. Figure 3c, d shows the cross-section images of the composite

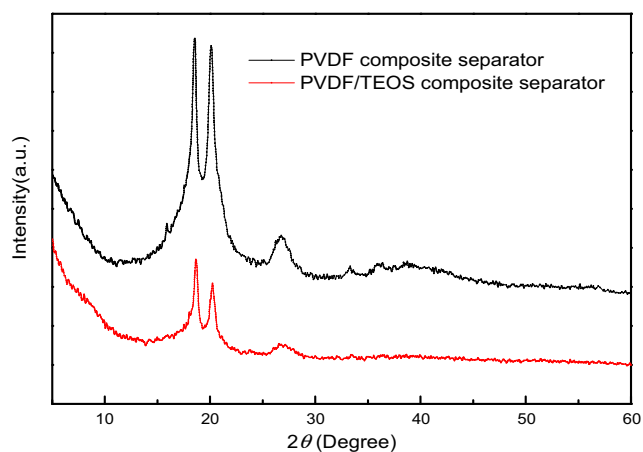


Fig. 4 XRD patterns of pristine PVDF and PVDF/TEOS composite separator

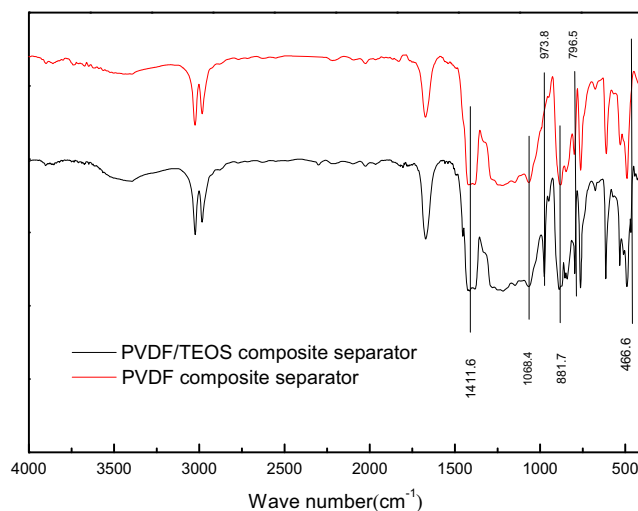


Fig. 5 FTIR spectrum of pristine PVDF and PVDF/TEOS composite separator

separator, which has an asymmetric structure with a thick finger-like pore layer and a thin skin layer. In general, the high DMAC concentration in coagulation bath would delay the liquid-liquid phase separation during the solvent and non-solvent exchange process and it is beneficial for the formation of a sponge-like pore [22]. But the finger-like pore forms in the composite separator, which may be because the porous substrate supports many channels for non-solvent and enhances the exchange rate of solvent and non-solvent.

To explore the effect of TEOS on the crystallinity of the PVDF separator, the XRD patterns of both pristine PVDF composite separator and PVDF/TEOS composite separator were investigated. As shown in Fig. 4, it can be noted that the diffraction peaks of 18.72°, 20.33°, and 26.72° can be indexed as  $\alpha$  phase of PVDF [23], and the diffraction peaks of PVDF/TEOS composite separator are much broader and the peaks are obviously weakened because the high dispersive TEOS disrupts the ordered crystal during the solvent and non-

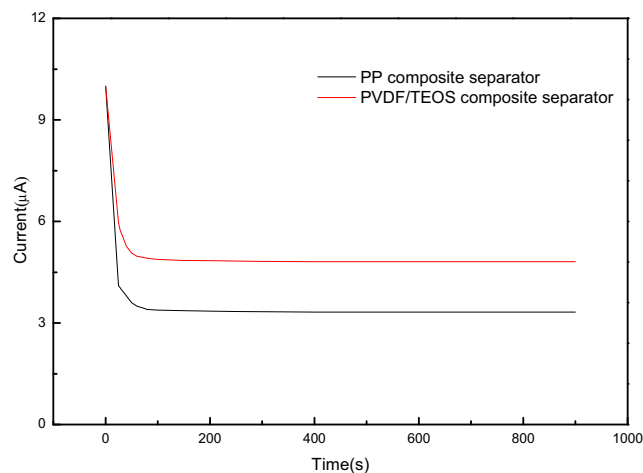
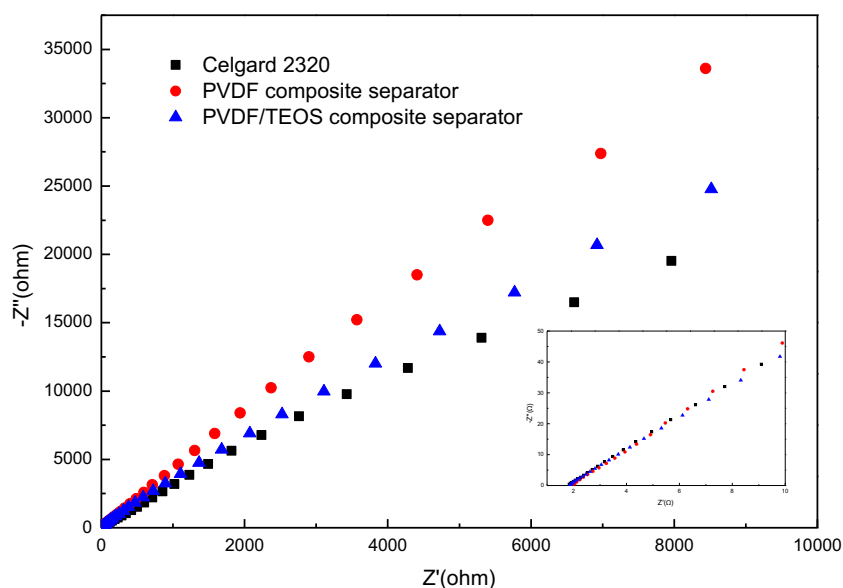


Fig. 6 Comparison of lithium-ion transference numbers of pristine PVDF and PVDF/TEOS composite separator

**Fig. 7** Electrochemical impedance spectrum of Celgard 2320 separator, pristine PVDF, and PVDF/TEOS composite separator



solvent exchange process, leading to the reduced crystallinity and the expanded amorphous area of PVDF/TEOS composite separator compared to the pristine PVDF composite separator.

Figure 5 is the FTIR spectrum of PVDF/TEOS and PVDF composite separator. The vibrational absorption peaks at  $1068.4\text{ cm}^{-1}$ ,  $1411.6\text{ cm}^{-1}$ ,  $796.5\text{ cm}^{-1}$ , and  $881.7\text{ cm}^{-1}$  respectively indicate the C–H bond linked with C–F bond in the PVDF segment, C–F bond, the absorption peak of crystalline phase and absorption peak of amorphous phase accordingly. As shown in Fig. 5, the above-mentioned four kinds of vibration absorption peaks exist in both the PVDF and PVDF/TEOS composite separator. However, the characteristic peaks appeared at  $466.6\text{ cm}^{-1}$  and  $973.8\text{ cm}^{-1}$  in the PVDF composite separator with TEOS added. It can be seen from the literature that these are the vibrational absorption peaks of Si–O–Si and Si–OH, respectively [24]. Combined with SEM and XRD analysis results, it can be concluded that TEOS decomposes with water in the phase separation process, but its decomposition product is too small or amorphous, resulting in the absence of decomposition products in the SEM and XRD results.

The lithium-ion transference number is the percentage of charge provided by lithium-ion migration during the cycling of a lithium-ion battery over all ion transport charges, so the value of the transport number is always less than 1. It is not sufficient to evaluate the effect of Li-ion battery separators on the battery's rate performance depending on ionic conductivity

alone, because ionic conductivity includes the contribution of both anions and cations. Hence, the product of the ionic conductivity and the lithium-ion transference number is the indicator that truly reflects the speed of lithium-ion transport in the electrolyte-containing separator. Figure 6 shows a comparison of lithium-ion transference numbers for the PVDF composite separator with 0.7% TEOS added and Celgard 2400 separator. It can be calculated from Eq. 4 that the lithium-ion transference number of Celgard 2400 separator was 0.332, and the PVDF composite separator added 0.7% TEOS was 0.481. The lithium-ion transference number of the modified PVDF separator is significantly higher than that of Celgard 2400 separator. This is mainly due to the fact that the modified PVDF separator contains –C–F bond and Si–O–Si bond.

The AC impedance spectra of Celgard 2320, pristine PVDF, and PVDF/TEOS composite separator are illustrated in Fig. 7, respectively. It can be observed that the bulk resistance of Celgard 2320, pristine PVDF, and PVDF/TEOS composite separators is 1.84, 1.94, and 1.86  $\Omega$ , respectively. According to Eq. (1), the calculated ionic conductivity of Celgard 2320, pristine PVDF, and PVDF/TEOS composite separator are 0.88, 1.17, 1.22  $\text{mS cm}^{-1}$ , respectively, integrated with the thickness of the membrane shown in Table 1 and the area of the blocking electrode. The enhanced ionic conductivity and low internal resistance of PVDF composite separator with the finger-like pore structure will attribute to reduce the distance of the lithium-ion

**Table 1** Ionic conductivity and liquid uptake of different separators

Properties	Celgard 2320	PVDF composite separator	PVDF/TEOS composite separator
Thickness ( $\mu\text{m}$ )	20	35	35
Liquid uptake (%)	75	160	200
Ionic conductivity ( $\text{mS cm}^{-1}$ )	0.88	1.17	1.22

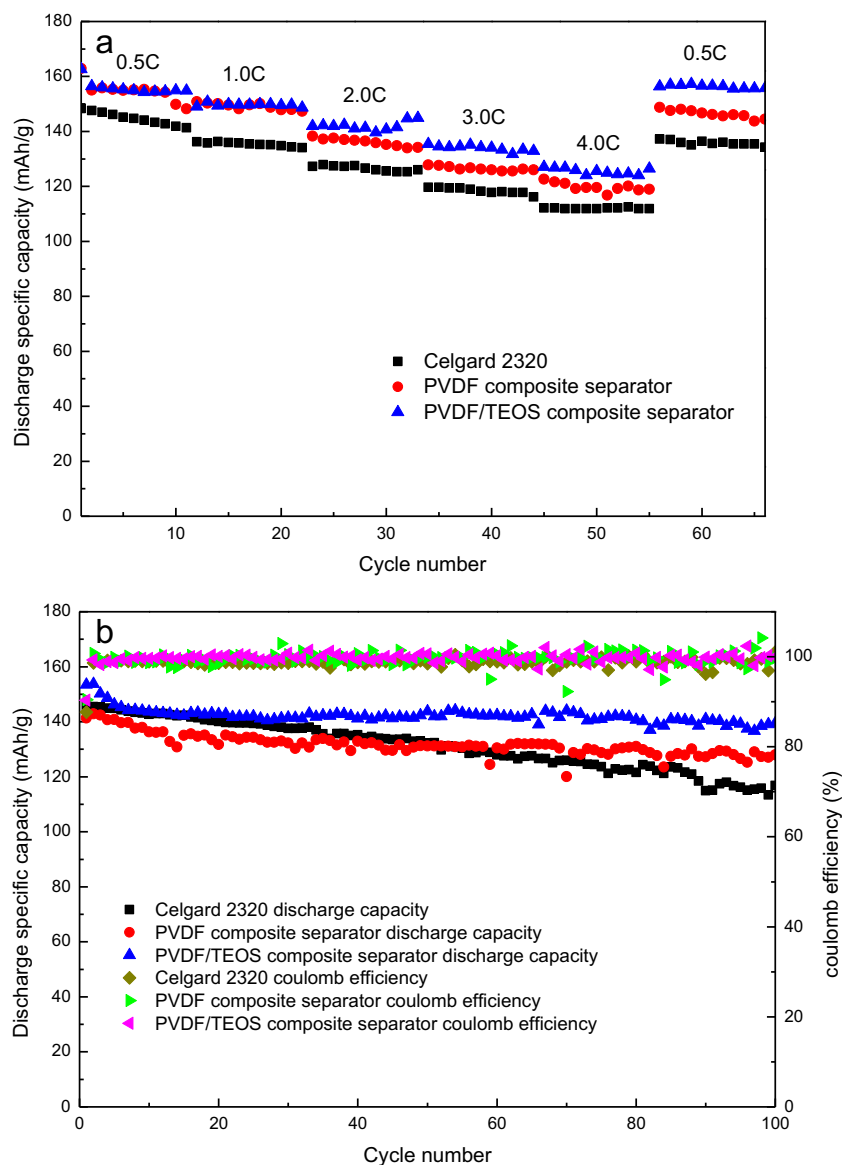


**Fig. 8** Rate capability (a) and cycling performance and coulombic efficiency (b) of Celgard 2320 separator, pristine PVDF, and PVDF/TEOS composite separator, respectively

migration in the separator and expand amorphous area which is easily swollen by electrolyte [25]. However, under the condition of using the same electrolyte solution, the ionic conductivity of PVDF-HFP composite separator with  $\text{TiO}_2$ , NaY, and SBA-15 added are  $0.9 \cdot 10^{-3}$ ,  $0.5 \text{ mS cm}^{-1}$ , respectively [26].

Figure 8a depicts the C-rate profiles of Celgard 2320 and the composite separators, wherein the discharge specific capacity of PVDF/TEOS composite separator at 0.5 C, 1.0 C, 2.0 C, 3.0 C, and 4.0 C rate is 154.9, 148.6, 144.8, 132.9, and 126.5  $\text{mAh g}^{-1}$ , respectively, which are higher than those of Celgard 2320 and pristine PVDF composite separator. This is because the novel finger-like PVDF layer provides the adequate liquid electrolyte retention and uniform pore distribution. At the same time, the PVDF amorphous area absorbs the mass of electrolyte and improves the wettability of separator.

The cycling performance of the different separators are summarized and compared in Fig. 8b. The discharge capacity retention after the 100th cycle is found to be 90.0% for the PVDF composite separator, 90.2% for the PVDF/TOES composite separator, and 79.3% for Celgard 2320 separator, respectively. This excellent cycling performance of the PVDF/TOES composite separator may be ascribed to its highly developed porous structure, better affinity for liquid electrolyte, and good electrolyte retention during cycling.

## Conclusions

PVDF/TEOS composite separator with the novel finger-like structure was successfully prepared via NIPS. The PVDF/

TEOS composite separator has ion conductivity of  $1.22 \text{ mS cm}^{-1}$  at  $25^\circ\text{C}$  and the lithium-ion batteries assembled with the PVDF/TEOS composite separator exhibit good cycling performance and rate capability compared with the commercial separator. Hence, the facile preparation of PVDF/TEOS composite separator provides a method to modify the commercial separator for lithium-ion battery.

**Funding information** The authors received financial support from The National Key R&D Program of China (Grant no. 2018YFB0104203).

**Open Access** This article is distributed under the terms of the Creative Commons Attribution 4.0 International License (<http://creativecommons.org/licenses/by/4.0/>), which permits unrestricted use, distribution, and reproduction in any medium, provided you give appropriate credit to the original author(s) and the source, provide a link to the Creative Commons license, and indicate if changes were made.

## References

- Li Y, Xu G, Yao Y, Xue L, Yanilmaz M, Lee H, Zhang X (2014) Coaxial electrospun Si/C–C core–shell composite nanofibers as binder-free anodes for lithium-ion batteries. *Solid State Ionics* 258:67–73
- Lee H, Yanilmaz M, Toprakci O, Fu K, Zhang X (2014) A review of recent developments in membrane separators for rechargeable lithium-ion batteries. *Energy Environ Sci* 7(12):3857–3886
- Liu JQ, He CF, He JY, Cui JQ, Liu HX, Wu XF (2017) An enhanced poly(vinylidene fluoride) matrix separator with high density polyethylene for good performance lithium ion batteries. *J Solid State Electrochem* 21(4):919–925
- Tarascon JM, Armand M (2001) Issues and challenges facing rechargeable lithium batteries. *Nature* 414(6861):359–367
- Yang P, Zhang P, Shi C, Chen L, Dai J, Zhao J (2015) The functional separator coated with core–shell structured silica–poly(methyl methacrylate) submicrospheres for lithium-ion batteries. *J Membr Sci* 474:148–155
- Cho W, Kim SM, Song JH, Yim T, Woo SG, Lee KW, Kim JS, Kim YJ (2015) Improved electrochemical and thermal properties of nickel rich  $\text{LiNi}_{0.6}\text{Co}_{0.2}\text{Mn}_{0.2}\text{O}_2$  cathode materials by  $\text{SiO}_{0.2}$  coating. *J Power Sources* 282:45–50
- Levi MD, Salitra G, Markovsky B, Teller H, Aurbach D, Heider U, Heider L (1999) Solid-state electrochemical kinetics of Li-ion intercalation into  $\text{Li}_{1-x}\text{CoO}_2$ : simultaneous application of electroanalytical techniques SSCV, PITT, and EIS. *J Electrochem Soc* 146(4):1279–1289
- Ma Y, Li LB, Gao GX, Yang XY, You J, Yang PX (2016) Ionic conductivity enhancement in gel polymer electrolyte membrane with N-methyl-N-butyl-piperidinebis(trifluoromethylsulfonyl) imide ionic liquid for lithium ion battery. *Colloids Surf, A* 502:130–138
- Zaghib K, Dontigny M, Guerfi A, Charest P, Rodrigues I, Mauger A, Julien CM (2011) Safe and fast-charging Li-ion battery with long shelf life for power applications. *J Power Sources* 196(8):3949–3954
- Liang X, Yang Y, Jin X, Cheng J (2016) Polyethylene oxide-coated electrospun polyimide fibrous separator for high-performance lithium-ion battery. *J Mater Sci Technol* 32(3):200–206
- Liao HY, Zhang HY, Hong HQ, Li ZH, Lin YX, Zhu HP, Qin G (2016) Novel cellulose aerogel coated on polypropylene separators as gel polymer electrolyte with high ionic conductivity for lithium-ion batteries. *J Membr Sci* 514:332–339
- Gopalan AI, Santhosh P, Manesh KM, Nho JH, Kim SH, Hwang CG, Lee KP (2008) Development of electrospun PVdF–PAN membrane-based polymer electrolytes for lithium batteries. *J Membr Sci* 325(2):683–690
- Yanilmaz M, Chen C, Zhang XW (2013) Fabrication and characterization of SiO/PVDF composite nanofiber-coated PP nonwoven separators for lithium-ion batteries. *J Polym Sci Part B: Polym Phys* 51:1719–1726
- Lalia BS, Samad YA, Hashaikeh R (2013) Nanocrystalline cellulose-reinforced composite mats for lithium-ion batteries: electrochemical and thermomechanical performance. *J Solid State Electrochem* 17(3):575–581
- Ding GL, Qin BS, Liu ZH, Zhang JJ, Zhang B, Hu P, Zhang CJ, Xu GJ, Yao JH, Cui JL (2015) A polyborate coated cellulose composite separator for high performance lithium ion batteries. *J Electrochem Soc* 162(6):A834–A838
- Xiao W, Miao C, Yin XQ, Zheng YC, Tian ML, Li H, Mei P (2014) Effect of urea as pore-forming agent on properties of poly(vinylidene fluoride-co-hexafluoropropylene)-based gel polymer electrolyte. *J Power Sources* 252:14–20
- Li H, Chen YM, Ma XT, Shi JL (2011) Gel polymer electrolytes based on active PVDF separator for lithium ion battery. I: Preparation and property of PVDF/poly(dimethylsiloxane) blending membrane. *J Membr Sci* 379(1–2):397–402
- Zhang HP, Zhang P, Li ZH, Sun M, Wu YP, Wu HQ (2007) A novel sandwiched membrane as polymer electrolyte for lithium ion battery. *Electrochem Commun* 9:1700–1703, 7
- Kim J, Seo J, Bae JY (2009) Preparation and characterization of chemical gel based on [Epoxy/PEG/PVdF-HFP] blend for lithium polymer battery applications. *Polym Korea* 33:544–550
- Ma T, Cui Z, Wu Y, Qin S, Wang H, Yan F, Han N, Li J (2013) Preparation of PVDF based blend microporous membranes for lithium ion batteries by thermally induced phase separation: I. Effect of PMMA on the membrane formation process and the properties. *J Membr Sci* 444:213–222
- Lloyd DR, Kim SS, Kinzer KE (1990) Microporous membrane formation via thermally induced phase separation. I. Solid-liquid phase separation. *J Membr Sci* 52(3):239–261
- Gregorio R (2006) Determination of the  $\alpha$ ,  $\beta$ , and  $\gamma$  crystalline phases of poly(vinylidene fluoride) films prepared at different conditions. *J Appl Polym Sci* 100(4):3272–3279
- Chen T, Liao Y, Wang X, Luo X, Li X, Li W (2016) Investigation on high-safety lithium ion battery using polyethylene supported poly(methyl methacrylateacrylonitrile-butyl acrylate) copolymer based gel electrolyte. *Electrochim Acta* 191:923–932
- Lima KO, Biduski B (2017) Incorporation of tetraethylorthosilicate (TEOS) in biodegradable films based on bean starch (*Phaseolus vulgaris*). *Eur Polym J* 154:A649–A655
- Yang CM, Kim HS, Na BK, Kum KS, Cho BW (2006) Gel-type polymer electrolytes with different types of ceramic fillers and lithium salts for lithium-ion polymer batteries. *J Power Sources* 156(2):574–580
- Nunes-Pereira J, Costa CM, Lanceros-Méndez S (2015) Polymer composites and blends for battery separators: State of the art, challenges and future trends. *J Power Sources* 281:378–398